Progress In Electromagnetics Research Letters, Vol. 65, 95–102, 2017

A Compact Wideband Circularly Polarized L-Slot Antenna Edge-Fed by a Microstrip Feedline for C-Band Applications

Mubarak S. Ellis, Jerry J. Kponyo, and Abdul-Rahman Ahmed

Abstract—A compact circularly polarized antenna using a wide L-shaped slot and a microstrip feedline is proposed. The measured results demonstrate that the antenna has an axial ratio (AR) $< 3\,\mathrm{dB}$ bandwidth ranging from 5–8.5 GHz and an $S_{11} < -10\,\mathrm{dB}$ bandwidth ranging from 4–8.6 GHz. The antenna is very simple, composed of an L-slot and a microstrip feedline placed beneath and to the edge of the L-slot. The size of the antenna is $20 \times 20\,\mathrm{mm}^2$ which is attractive for compact wireless devices that operate in C-band. The antenna has very low cost and does not require: a large size, truncated corners, reflecting surfaces, complex feeding structure, and via connections, which increase fabrication cost and design complexity.

1. INTRODUCTION

Circular polarization (CP) has become more popular in modern mobile wireless communications systems. The advantages of CP schemes are more evident in direct satellite-to-land communications since CP is more immune to bad weather conditions and less sensitive to the orientation of the corresponding mobile device. Wideband circular polarization is desirable in most applications. There are several design techniques proposed to achieve wideband circular polarization.

One of the techniques proposed is to arrange the antenna elements in a sequential rotation array configuration [1, 2]. This technique significantly improves the AR bandwidth, but the design requires additional circuit components such as a wideband power divider with phase quadrature and a much larger circuit board. Another technique which has gained a lot of recognition is using printed wide-slot antennas because of their wider impedance bandwidths than microstrip antennas. The most commonly used wide-slot antennas are the circularly polarized square-slot antennas (CPSSA). Several CPSSAs have been proposed to achieve CP [3–7]. The CP operations of these antennas are achieved by introducing perturbations into the wide slot in the form of feedline [3, 4], slot structure [5, 6], and array configuration [7]. However, antenna configurations of these designs are so complicated that they lead to complexity in antenna design and fabrication. An L-shaped wide-slot circularly polarized antenna has also been introduced [8–11]. In [8] and [9], the CP operation was achieved by introducing a feedline perturbation in the form of an L-probe feed connected to an L-shaped slot through a shorting via connector. Additionally, the corner of the antenna was truncated to introduce extra perturbation to enhance the CP performance. High cross-polarization was also achieved and stated in [9] that its reduction was subject to further study. In [10], CP operation was achieved by using an open L-slot and a C-shaped microstrip line. However, proper design and orientation of the C-shaped feedline to achieve CP operation will prove difficult. Even though lower cross-polarization was achieved than [8] and [9], a relatively small axial ratio (AR) bandwidth (400 MHz) was achieved. In [11], a combination of an L-slot and a rectangular slot was also proposed to achieve a wide AR bandwidth. The size of this

Received 11 November 2016, Accepted 5 January 2017, Scheduled 19 January 2017
* Corresponding author: Mubarak Sani Ellis (smellis.coe@knust.edu.gh).
The authors are with the Department of Electrical & Electronic Engineering, Kwame Nkrumah University of Science and Technology, Ghana.

antenna is $41 \times 41\,\text{mm}^2$ and achieves an $S_{11} < -10\,\text{dB}$ bandwidth from 4–8 GHz, and an AR bandwidth of 3.7–8.2 GHz.

In this work, a new wide-slot antenna is proposed. The proposed antenna consists of an unsymmetrical L-shaped slot created on a ground plane and a microstrip feedline placed underneath the right side of the L-shaped slot. The CP operation is achieved without adding perturbations inside the slot and on the feedline as compared to techniques in [1–10]. Additionally, a wide AR bandwidth of 3.45 GHz is achieved with a small and compact size of $20 \times 20\,\text{mm}^2$ without using: a truncated corner, a reflector surface, or any connecting via for the feedline [8, 9]. Compared to [11], the proposed antenna uses half the size in [11] to achieve an even larger S_{11} bandwidth leading to a comparatively miniaturized design. Additionally, the AR bandwidth falls within the S_{11} bandwidth and also maintains a symmetric radiation patterns with low cross polarization, unlike in [11]. This makes it easy to fabricate at low cost for practical applications and also suitable for small and portable devices. Table 1 compares the proposed antenna and referenced antennas in terms of antenna size, AR center frequency, and fractional AR bandwidth. It can be noticed that the different antennas have areas where they are more advantageous than others, in terms of size and AR bandwidth.

Table 1. Comparison of the proposed antenna with other square slot Refs. [3–7] and L-shaped slot Refs. [8–11] CP antennas.

Ref. antennas	Antenna Area (mm^2)	f_c (MHz)	3-dB ARBW (%)
3	60×60	2220	30.6
5	60×60	2165	32.8
6	60×50	2365	8.8
[8, 9]	82×82	2840	46.5
[10]	70×70	1700	23.5
[11]	41×41	6005	74.4
This work	20×20	6750	51.8

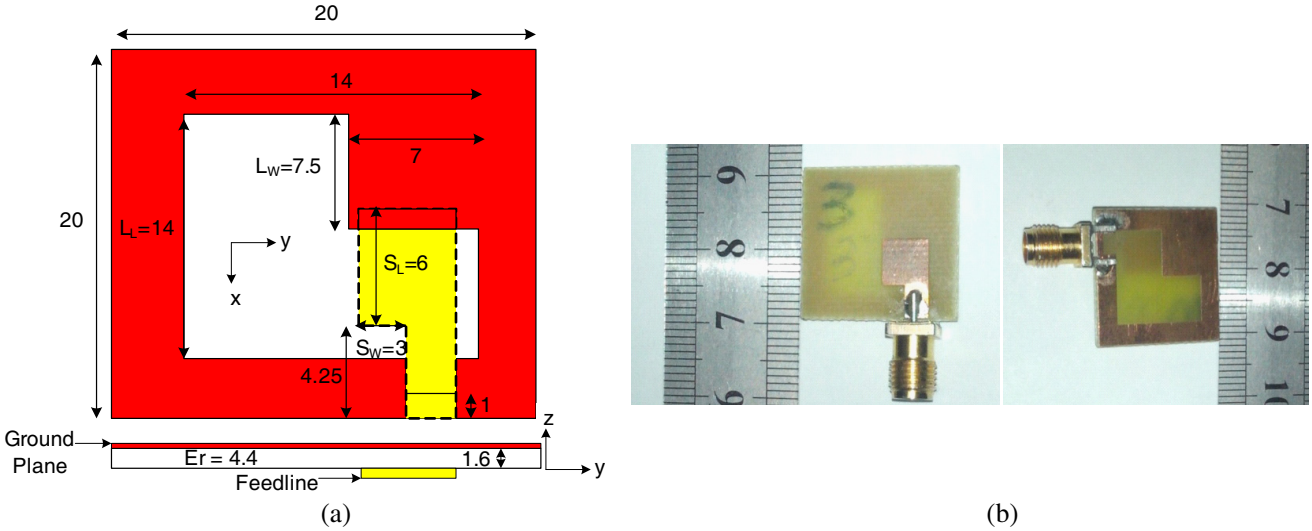

Figure 1. Picture showing: (a) Geometry of the proposed antenna, (b) fabricated prototype.

2. ANTENNA STRUCTURE AND DESIGN

The proposed antenna is shown in Fig. 1. As shown in the figure, the proposed antenna is fed by a 50 Ohm microstrip feedline printed on the top part of an FR4 substrate with thickness 1.6 mm and relative permittivity of 4.4. The width of the feedline is 3 mm. The ground plane is printed on the bottom of the substrate. A large L-slot is created in the ground plane of the antenna. The L-shaped structure generates electric fields between the ground plane structures around each slot (vertical and horizontal parts) [10]. Therefore, by designing an appropriate feedline and adjusting the shape of the L-slot, a 90° phase difference between these two orthogonal electric fields over the band of interest is created. In Section 3, the effect of different parameters on the reflection coefficient and AR is discussed. A gap is created on the ground plane above the feedline to reduce the coupling between the feedline and the ground plane. The overall size is $20 \times 20\,\text{mm}^2$ which is suitable for small and compact mobile devices. The antenna is printed on the xoy axis.

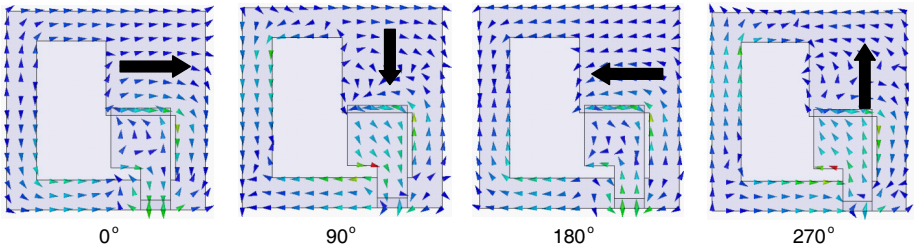

Figure 2. Distribution of surface current at 7.2 GHz at 0°, 90°, 180°, and 270°.

3. SIMULATIONS AND MEASUREMENTS

The proposed antenna is simulated using Ansoft commercial high frequency structure simulator (HFSS) software. The simulated and measured S_{11} and AR plots are shown in Figs. 3(a) and 3(b), respectively. The measured results show an impedance bandwidth of 4–8.6 GHz ($S_{11} < -10$ dB). The discrepancy between the simulated and measured results may be due to the attached SMA connector and fabrication imperfections. The AR plots show good agreement between simulated and measured results and presents a 3.5 GHz AR bandwidth ranging from 5–8.5 GHz (AR < 3 dB). The AR and impedance bandwidths overlap with each other perfectly. This wide AR bandwidth in the proposed antenna is achieved without using: a reflector surface, a large antenna size, complex probe feeding, complicated feed, and truncations — resulting in a simple and compact design. The measured and simulated peak gains in the AR bandwidth are shown in Fig. 4. A peak gain between 2–5 dBi is achieved within the AR band.

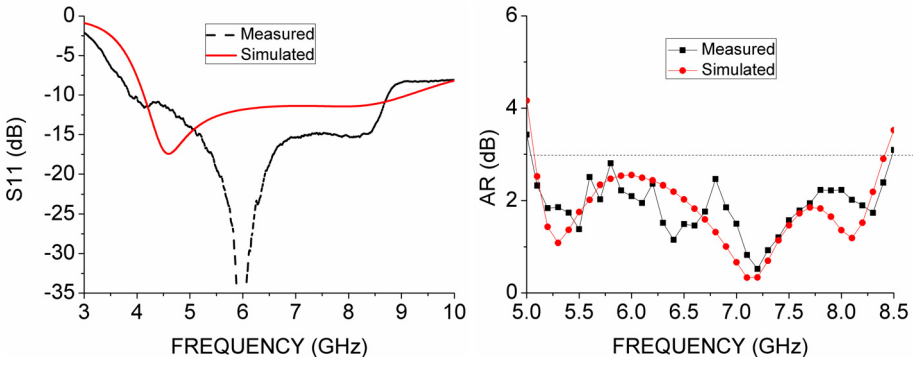

Figure 3. Simulated and measured. (a) S_{11}. (b) Axial ratio.

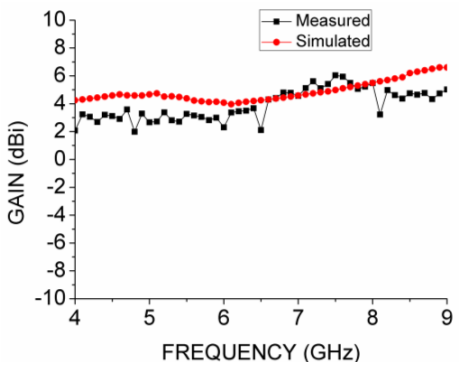

Figure 4. Peak gain of the proposed antenna within the AR bandwidth.

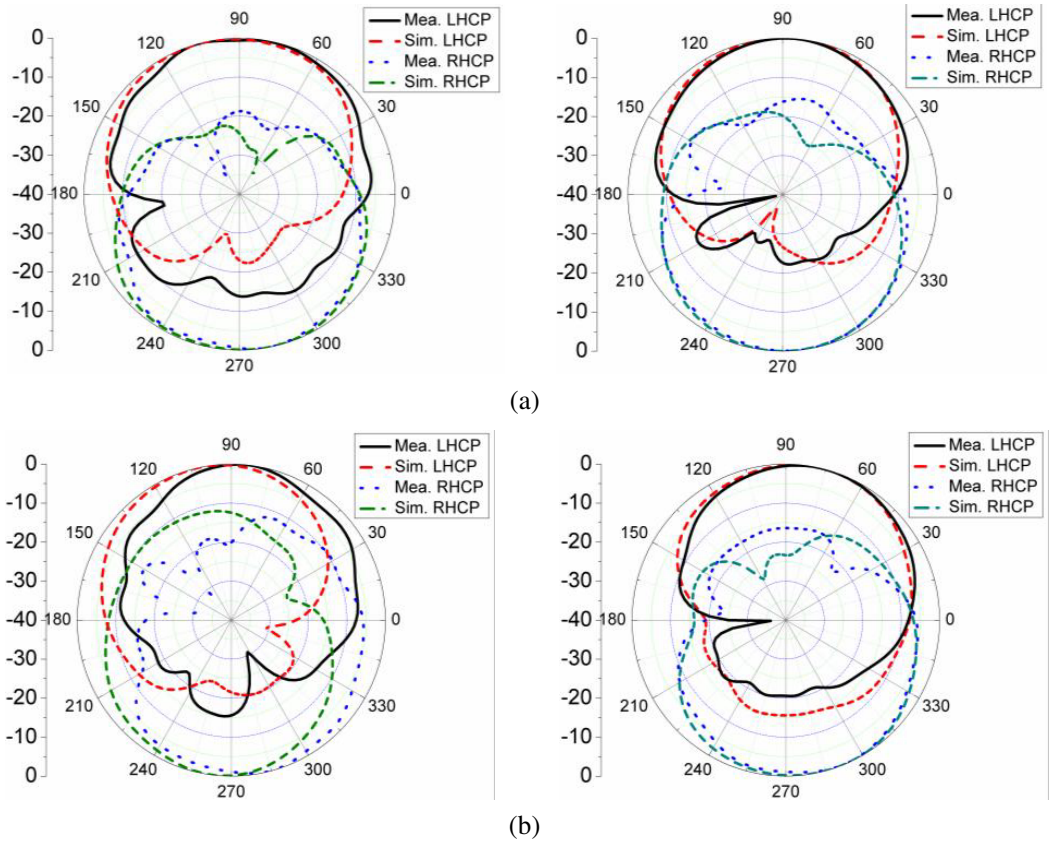

Figure 5. Measured radiation pattern at xoz (left) and yoz (right) planes at: (a) 6 GHz, (b) 7 GHz.

The simulated and measured radiation patterns at 6 GHz and 7 GHz are shown in Fig. 5. It is shown that the antenna exhibits left-hand circular polarization (LHCP) in the $z > 0$ space and right-hand circular polarization (RHCP) in the $z < 0$ spaces. This is illustrated in Fig. 2 which shows the simulated time-varying surface current distribution at 7.2 GHz. This frequency is the minimum point of the AR. It is observed that the surface current distributions at 180° and 270° are equal in magnitude and opposite in phase to 0° and 90°. This shows that the proposed antenna exhibits LHCP in the $+z$ direction whereas a RHCP is produced in the $-z$ direction. The radiation patterns are measured at two different frequencies within the AR bandwidth, i.e., 6 GHz and 7 GHz in both xoz and yoz planes. The 3D polar plots of the radiation patterns at the measured frequencies are also depicted in Fig. 6 to demonstrate the LHCP at $+z$ directions and RHCP at $-z$ directions. Fig. 7 also shows the 3D polar

Figure 6. 3D radiation patterns at LHCP (left) and RHCP (right) planes at: (a) 6 GHz, (b) 7 GHz.

Figure 7. 3D radiation patterns at LHCP (left) and RHCP (right) planes at: (a) 5 GHz, (b) 8 GHz.

plots for 5 GHz and 8 GHz to prove that the entire AR frequencies radiate circularly polarized waves. In each figure, the LHCP only shows maximum electric field strength in the $+z$ direction of the antenna with minimum radiation in the $-z$ direction. Similarly, RHCP also shows maximum electric field in the $-z$ directions and minimum electric field in the $+z$ directions as expected.

4. PARAMETRIC ANALYSIS

In this section, the results of parametric studies on the proposed antenna are presented. The parameters considered are the length (S_L) and width (S_W) of the stub added on the feedline, the length (L_W) of one side of the L-shaped slot and the overall length/width (L_L) of the wide slot. For each varying parameter, the other dimensions are fixed to the values indicated in Fig. 1. The simulation results are discussed to provide knowledge on how the antenna's performance in terms of S_{11} and AR are affected by each varying parameter.

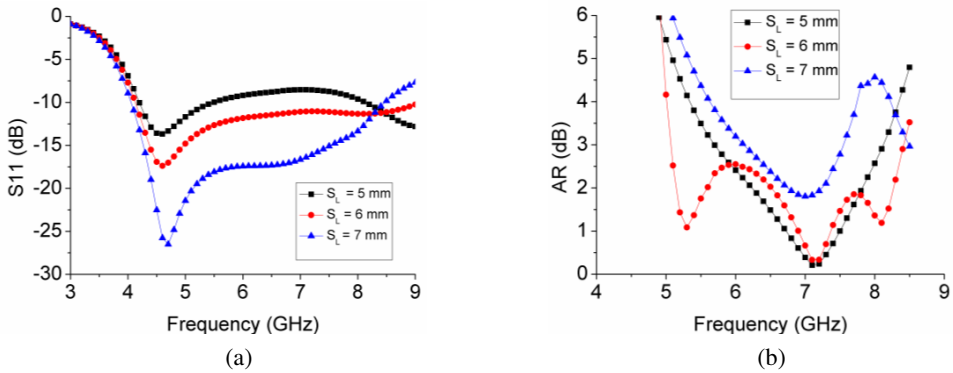

Figure 8. Effect of stub length S_L on S_{11} and AR.

4.1. Effect of S_L

The results of different values of S_L on AR and S_{11} are shown in Figs. 8(a) and (b). It can be noticed that the stub has significant effect on the reflection coefficient. S_{11} is seen to improve when S_L increases towards the $+x$ direction. This is possibly because when S_L is small, only a little section of the slot is excited (the top part of the horizontal slot), hence the total slot is not properly excited enough to properly realize an efficient radiator. However, when the stub length increases, the bottom part of the L-shaped slot is properly excited due to adequate coupling, and S_{11} is greatly improved. It should be noted however that, when $S_L = 7\,\text{mm}$, a very good S_{11} is achieved, but the high frequency above 8 GHz slightly worsens. Therefore, a trade-off needs to be made when choosing S_L. The AR plot in Fig. 8(b) shows that a large AR bandwidth is achieved when $S_L = 5\,\text{mm}$. The bandwidth is further improved when $S_L = 6\,\text{mm}$. When $S_L = 7\,\text{mm}$ however, a significantly lower bandwidth is achieved.

4.2. Effect of S_W

The effect of S_W on AR and S_{11} bandwidths is demonstrated in Figs. 9(a) and (b). It can be noted from Fig. 9(a) that an increase in S_W value towards $-y$ direction improves S_{11} accordingly. The S_{11} values slightly improve across the entire frequency when S_W increases from 2 mm to 4 mm. In the AR plot however, when $S_W = 2\,\text{mm}$, a large AR bandwidth is achieved except at 6 GHz where the AR level is noticed to be greater than 3 dB. When $S_W = 3\,\text{mm}$, an increased AR bandwidth is achieved with all relevant frequencies under 3 dB. When S_W is further increased to $S_W = 4\,\text{mm}$, a significant reduction in bandwidth is realized.

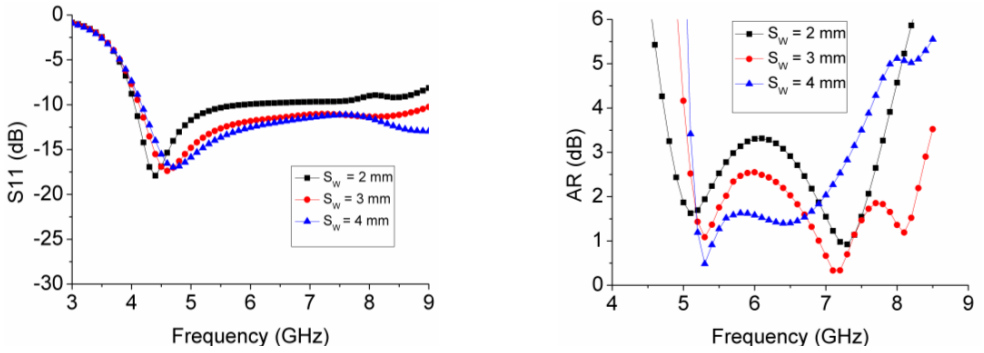

(a) (b)

Figure 9. Effect of stub length S_W on S_{11} and AR.

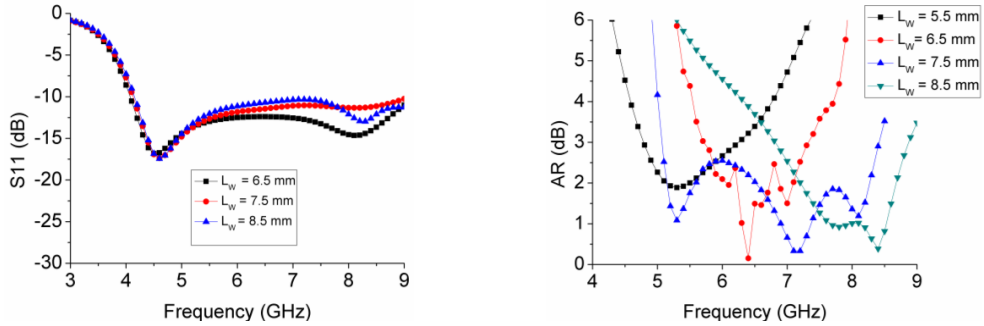

(a) (b)

Figure 10. Effect of slot length L_W on S_{11} and AR.

4.3. Effect of L_W

Figures 10(a) and (b) demonstrate the effect of L_W on AR and S_{11} of the antenna. When L_W is increased, there is only a slight change in S_{11}. This change is noticed around 8 GHz where a second resonance is noticed to appear. Therefore, it can be said that changes in the slot size, which is also a measure of the ground plane size, can introduce a second resonance in the S_{11} plot. This may explain the almost-unnoticeable second resonance that seems to appear in the measured S_{11} results at around 8 GHz in Fig. 3(a) due to the SMA connector. By attaching the SMA connector and RF measurement cable, the size of the ground may electrically increase, and this may cause the second resonance to appear, as shown in Fig. 10(a). The AR plot is also shown, and it can be noticed that when $L_W = 5.5$ mm, a relatively lower AR bandwidth is achieved. When $L_W = 6.5$ mm, there is a shift in the AR bandwidth to a higher frequency. The same phenomenon is noticed when $L_W = 8.5$ mm, with all three having almost the same bandwidth. When $L_W = 7.5$ mm however, a very wide AR bandwidth is achieved covering almost three bandwidths achieved when $L_W = 5.5$ mm, 6.5 mm, and 8.5 mm.

4.4. Effect of L_L

Figures 11(a) and 11(b) demonstrate the effect of L_L on AR and S_{11} of the antenna. It should be noted that since the slot is a square, a change in L_L corresponds to a change in both the width and length of the slot. When L_L is increased from 13 mm to 15 mm, the S_{11} plot starts to worsen. For instance, at 15 mm, frequencies between 5.5 GHz–7.5 GHz are less than the −10 dB threshold. The bandwidth is however the same for all three values. In contrast, the AR plot shows the least AR bandwidth when L_L is 13 mm and the best AR bandwidth when L_L is 14 mm. The optimum performance for both AR and S_{11} is achieved when L_L is 14 mm.

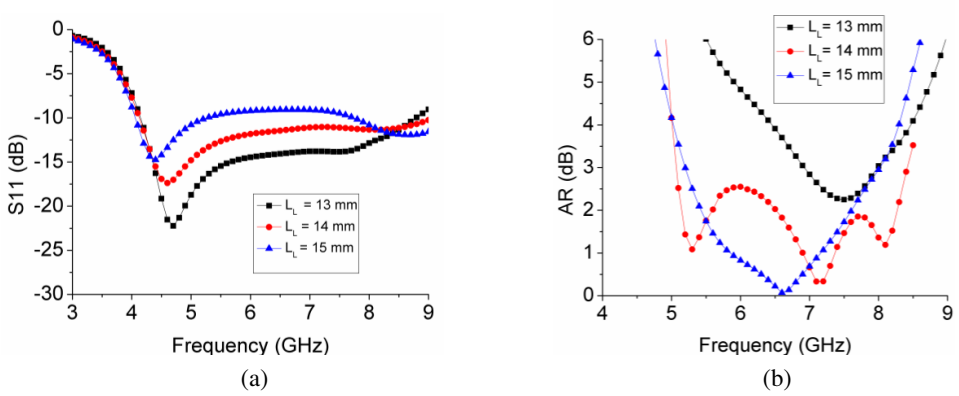

(a) (b)

Figure 11. Effect of slot length L_L on S_{11} and AR.

5. CONCLUSION

A low profile, low cost, L-shaped monopole slot antenna with a microstrip feedline is introduced in this work. The simulation and measurement results show that the antenna can achieve a broadband AR bandwidth from 5–8.5 GHz (51.9% fractional bandwidth) and an impedance bandwidth from 4–8.6 GHz (73% fractional bandwidth). The antenna is simple and compact, achieves a very wide AR bandwidth, and does not require any truncated corner, reflector surface, via connections, and complicated feeding mechanism unlike other L-slot CP antennas. This results in a significant reduction in circuit board fabrication and cost. Parametric studies were conducted, which identified the sensitive design parameters affecting the AR and reflection coefficient. The proposed antenna can be used in C-band LEO satellite applications including WLAN applications (5.5–6.3 GHz).

REFERENCES

1. Huang, J., "A technique for an array to generate circular polarization with linearly polarized elements," *IEEE Trans. Antennas Propag.*, Vol. 34, 1113–1124, Sep. 1986.
2. Yang, S. L. S., R. Chair, A. A. Kishk, K. F. Lee, and K. M. Luk, "Study of sequential feeding networks for subarrays of circularly polarized elliptical dielectric resonator antenna," *IEEE Trans. Antennas Propag.*, Vol. 55, No. 2, 321–333, Feb. 2007.
3. Chang, T. N., "Circular polarized antenna for 2.3–2.7 GHz WiMAX band," *Microw. Opt. Technol. Lett.*, Vol. 51, No. 12, 2921–2923, 2009.
4. Sze, J. Y., J. C. Wang, and C. C. Chang, "Axial-ratio bandwidth enhancement of asymmetric-CPW-fed circularly-polarised square slot antenna," *Electron. Lett.*, Vol. 44, No. 18, 1048–1049, Aug. 2008.
5. Chu, Q. X. and S. Du, "A CPW-fed broadband circularly polarized square slot antenna," *Microw. Opt. Technol. Lett.*, Vol. 52, No. 2, 409–412, Feb. 2013.
6. Wang, C.-J. and C.-M. Lin, "A CPW-Fed open-slot antenna for multiple wireless communications systems," *IEEE Antennas Wireless Propag. Lett.*, Vol. 11, 620–623, 2012.
7. Pourahmadazar, J. and V. Rafii, "Broadband circularly polarised slot antenna array for L and S-band applications," *Electron. Lett.*, Vol. 48, No. 10, 542–543, May 2012.
8. Yang, S. L. S., A. Kishk, and K. F. Lee, "Wideband circularly polarized antenna with L-shaped slot," *IEEE Trans. Antennas Propag.*, Vol. 56, No. 6, 1780–1783, Jun. 2008.
9. Muramoto, Y. and T. Fukusako, "Circularly polarized broadband antenna with L-shaped probe and L-shaped wide-slot," *Proc. Asia-Pacific Microwave Conf.*, 1–4, 2007.
10. Mousavi, P., B. Miners, and O. Basir, "Wideband L-shaped circular polarized monopole slot antenna," *IEEE Antennas Wireless Propag. Lett.*, Vol. 9, 822–825, 2010.
11. Nakao, S., R. Joseph, and T. Fukusako, "A circularly polarized L-shaped and rectangular slot antenna with an L-shaped probe for wideband characteristics," *Proc. IEEE Asia-Pacific Microw. Conf.*, 734–734, Dec. 2010.